



Disproportionate control on aerosol burden by light rain

Yong Wang¹, Wenwen Xia¹, Xiaohong Liu², Shaocheng Xie³, Wuyin Lin⁴, Qi Tang³, Hsi-Yen Ma³, Yiquan Jiang⁵, Bin Wang^{1,6,7} and Guang J. Zhang⁸✉

Atmospheric aerosols are of great climatic and environmental importance due to their effects on the Earth's radiative energy balance and air quality. Aerosol concentrations are strongly influenced by rainfall via wet removal. Global climate models have been used to quantify their climate and health effects. However, they commonly suffer from a well-known problem of 'too much light rain and too little heavy rain'. The impact of simulated rainfall intensities on aerosol burden at the global scale is still unclear. Here we show that rainfall intensity has profound impacts on aerosol burden, and light rain has a disproportionate control on it. By improving the representation of convection, the light-rain (1–20 mm d⁻¹) frequency in two state-of-the-art global climate models is reduced. As a result, the aerosol burden is increased globally, especially over the tropics and subtropics, by as much as 0.3 in aerosol optical depth in tropical rain belts. It is attributed to the dominant contribution of light rain to the accumulated wet removal by its frequent occurrence despite its weak intensity. The implication of these findings is that understanding the nature of aerosol scavenging by rainfall is critical to aerosol–climate interaction and its impact on climate.

Aerosols can reflect and absorb solar radiation, as well as alter cloud albedo and lifetime by serving as cloud condensation nuclei and ice-nucleating particles^{1–3}. Thus, changes in aerosol concentration influence the planetary energy balance^{4,5}. The net impact of cloud radiative forcing from anthropogenic aerosols is to cool the Earth's surface. As estimated by the Intergovernmental Panel on Climate Change Fifth Assessment Report⁶, the anthropogenic aerosol cloud radiative forcing is -0.45 W m^{-2} with a 90% uncertainty range of 0 to -1.2 W m^{-2} , partially offsetting the warming from greenhouse gases (GHGs)⁷. In addition to aerosol radiative effects, aerosol-induced air quality deterioration can impact human health. Long-term exposures to particulate matters with diameters $<2.5 \mu\text{m}$ ($\text{PM}_{2.5}$) can elevate the risks of having cardiovascular and respiratory diseases, resulting in premature mortality^{8–12}.

Among the processes affecting the atmospheric aerosols, wet scavenging is a major sink for submicron particles, which occurs both in clouds by nucleation scavenging and below clouds by Brownian diffusion and impaction¹³. Both rain intensity and frequency impact the atmospheric aerosol burdens, especially $\text{PM}_{2.5}$ and its effects on air quality^{14–16}. The global mean rainfall is projected to increase in future climate, which is thus expected to reduce aerosol burdens^{17–19}. However, changes in rainfall intensity, frequency and storm track may compensate for potential increases of wet scavenging associated with a projected increase in rainfall¹⁹. Recent modelling studies suggest that GHG-induced warming may result in an overall increase of aerosol burden^{15,20–22}. It has been primarily attributed to decreased wet removal associated with decreasing rainfall over land due to reductions in lower-tropospheric humidity from enhanced land–sea warming contrast as climate warms^{23,24}.

Although global climate models (GCMs) have been widely used for investigating the impact of rainfall on aerosols and associated

radiative effects in current and future climates, how the deficiencies in simulated rainfall intensity spectrum influence aerosol burden is rarely discussed^{25,26}. A well-known problem in all GCMs is 'too much light rain and too little heavy rain' compared with observations, which remains unresolved in Coupled Model Intercomparison Project, Phase 6 (CMIP6) models²⁷. This can have a huge impact on the realism of the aerosol burden and distribution in simulated current climate and future climate projections if the efficiency of aerosol wet removal is sensitive to rainfall intensity.

Observation-validated rainfall intensity spectrum

The problem of too much light rain and too little heavy rain is largely eliminated in the National Center for Atmospheric Research Community Atmosphere Model version 5 (NCAR CAM5) (Methods), especially over the tropics (Fig. 1a) after a stochastic convective parameterization is introduced^{28–30}. It greatly reduces the frequency of rainfall events $<20 \text{ mm d}^{-1}$ and enhances the frequency of rainfall events $>20 \text{ mm d}^{-1}$ (the stochastic (STOC) convection simulation; see Supplementary Table 1 for experiment design). Related to the reduction of light-rain frequency, the distribution of rainfall amount (defined by daily cumulative rainfall) shifts towards heavier rain rates with a reduced peak contribution to the total rainfall (Fig. 2a). Thus, the stochastic convection scheme makes both the modelled rainfall intensity spectrum and the contribution from different rainfall intensities to the total rainfall amount in much better agreement with Tropical Rainfall Measuring Mission (TRMM) and Global Precipitation Measurement (GPM) observations (Methods). The spatial distribution of the simulated rainfall intensity is also improved²⁸. The decrease of the frequency of total rainfall events $<20 \text{ mm d}^{-1}$ over the tropics is predominantly from convective rainfall while both convective and large-scale

¹Ministry of Education Key Laboratory for Earth System Modeling and Department of Earth System Science, Tsinghua University, Beijing, China.

²Department of Atmospheric Sciences, Texas A&M University, College Station, TX, USA. ³Lawrence Livermore National Laboratory, Livermore, CA, USA.

⁴Brookhaven National Laboratory, Upton, NY, USA. ⁵CMA-NJU Joint Laboratory for Climate Prediction Studies, Institute for Climate and Global Change Research, School of Atmospheric Sciences, Nanjing University, Nanjing, China. ⁶State Key Laboratory of Numerical Modelling for Atmospheric Sciences and Geophysical Fluid Dynamics, Institute of Atmospheric Physics, Chinese Academy of Sciences, Beijing, China. ⁷College of Earth and Planetary Sciences, University of Chinese Academy of Sciences, Beijing, China. ⁸Scripps Institution of Oceanography, La Jolla, CA, USA. ✉e-mail: gizhang@ucsd.edu

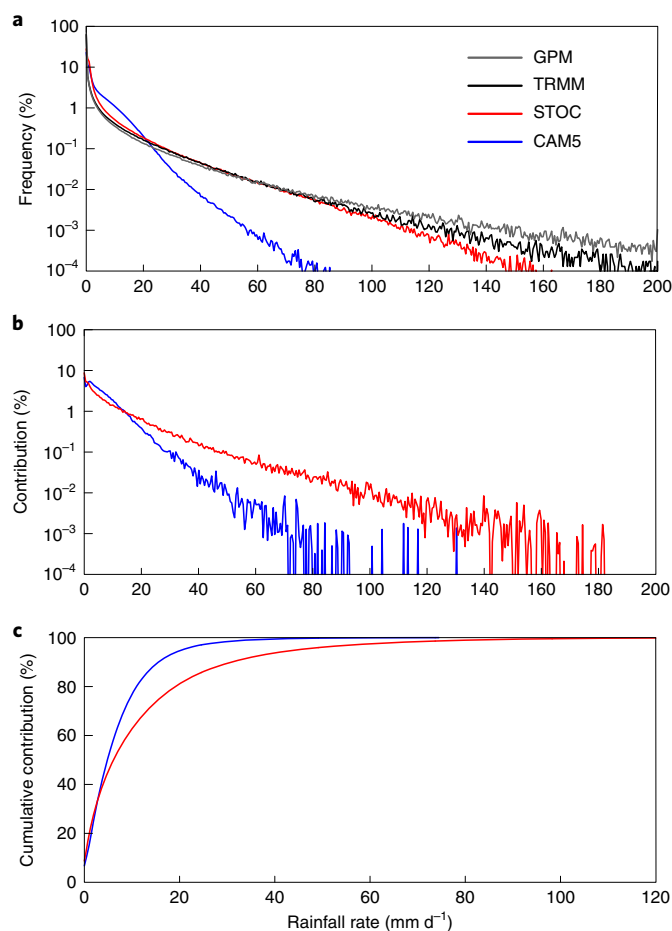


Fig. 1 | Rainfall intensity spectrum and aerosol wet removal as functions of rain rates. **a**, Frequency distributions of rainfall intensity over the tropics (20°S – 20°N) from GPM, TRMM observations, CAM5 and STOC simulations. **b,c**, Contributions of wet removal of aerosols (including all aerosol species) by different rainfall intensities to the total wet deposition (**b**) and cumulative contributions to wet removal (**c**) over the tropics (20°S – 20°N) in the CAM5 and STOC runs. Bin intervals of 0.5 mm d^{-1} are used for rainfall rates.

rainfall contribute to the increase of the frequency of the total rainfall events $>60\text{ mm d}^{-1}$ (Extended Data Fig. 1). By making convection occur less frequently^{28,31,32}, it allows the build-up of the atmospheric instability necessary to develop stronger convection and heavier rainfall³³. In addition to the improved rainfall intensity spectrum, other climate variables, including cloud radiative forcing, are also improved or comparable to those in the default model^{28,29,33} (Methods). A qualitatively similar change in the simulated rainfall intensity spectrum is also achieved in the US Department of Energy (DOE) Energy Exascale Earth System Model (E3SM) Atmosphere Model version 1 (EAMv1) (Methods and Extended Data Fig. 2). The improved rainfall intensity probability distribution function validated by observations provides a unique opportunity to explore its impact on aerosol burdens.

Reduced aerosol wet removal

The aerosol wet removal by rainfall varies approximately exponentially with rainfall intensity (Fig. 1b). Consequently, most of the wet removal is accomplished by light rain, with little contribution from intense rain. With an excessively high frequency of occurrence compared with observations, light rain in CAM5 plays a

disproportionate role in aerosol wet removal. For example, in the tropics, 77% of the total aerosol wet removal is done by rainfall rates $<10\text{ mm d}^{-1}$ and nearly 95% of the total wet removal is done by rainfall $<20\text{ mm d}^{-1}$ in CAM5 (Fig. 1c). It decreases to 63% by rainfall rates $<10\text{ mm d}^{-1}$ and 80% by rainfall $<20\text{ mm d}^{-1}$ after the light-rain frequency is reduced by using the stochastic convection parameterization (Fig. 1c). While both rainfall frequency and intensity can affect aerosol wet removal, the rain rates associated with the most rainfall contribution are larger than those corresponding to the most contribution to the total aerosol scavenging (comparing distribution peaks in Fig. 2a,b, Methods), which implies that rainfall frequency plays a more important role than rainfall intensity in regulating aerosol wet removal. The total amount of aerosol wet removal by different rainfall intensities decreases and the distribution shifts towards heavier rain rates. The tropical mean total aerosol wet removal is reduced from 18.8 to $16.1\text{ mg m}^{-2}\text{ d}^{-1}$ in the CAM5 model with the stochastic convection scheme (Fig. 2b). Over Northern Hemisphere midlatitudes where there is heavy emission of anthropogenic aerosols, the rightward shift of the distribution of rainfall amount (Extended Data Fig. 3a) and aerosol wet removal by different rainfall intensities (Extended Data Fig. 3b) are similar to those over the tropics although the reduction of the total

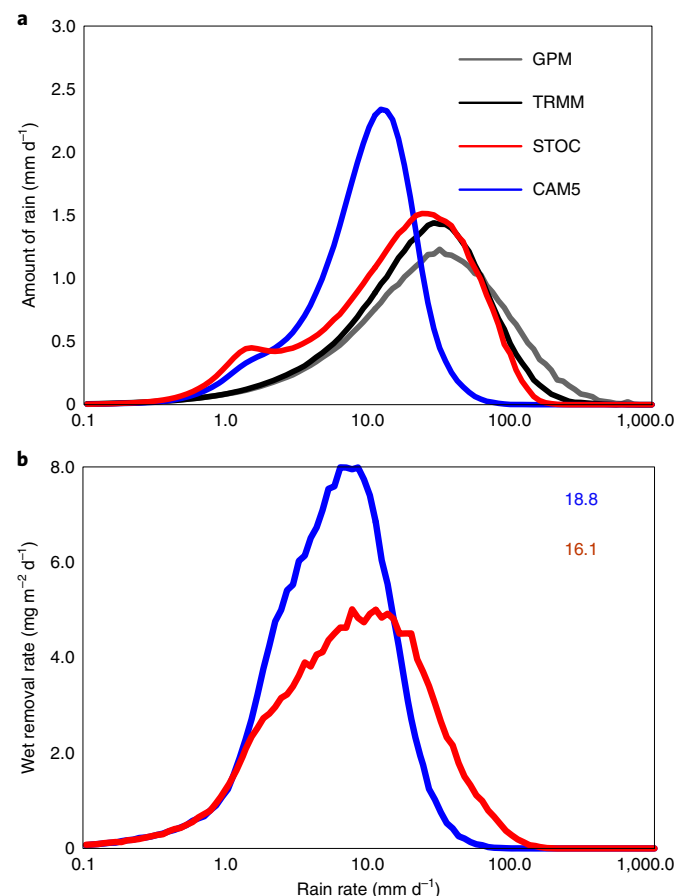


Fig. 2 | Rainfall and wet removal amount. **a,b**, Amount distributions of total daily rainfall (**a**) and wet removal of all aerosols (**b**) by different rainfall intensities over the tropics (20°S – 20°N). The total rainfall rate in the range from 0.1 to $1,000\text{ mm d}^{-1}$ is logarithmically scaled, with equal bin width of $\Delta \ln(R) = \Delta R/R = 0.1$, where R is rainfall rate and ΔR is the bin interval. Numbers in the right upper corner of **b** are regional mean aerosol wet deposition rates, which equal areas under respective curves.

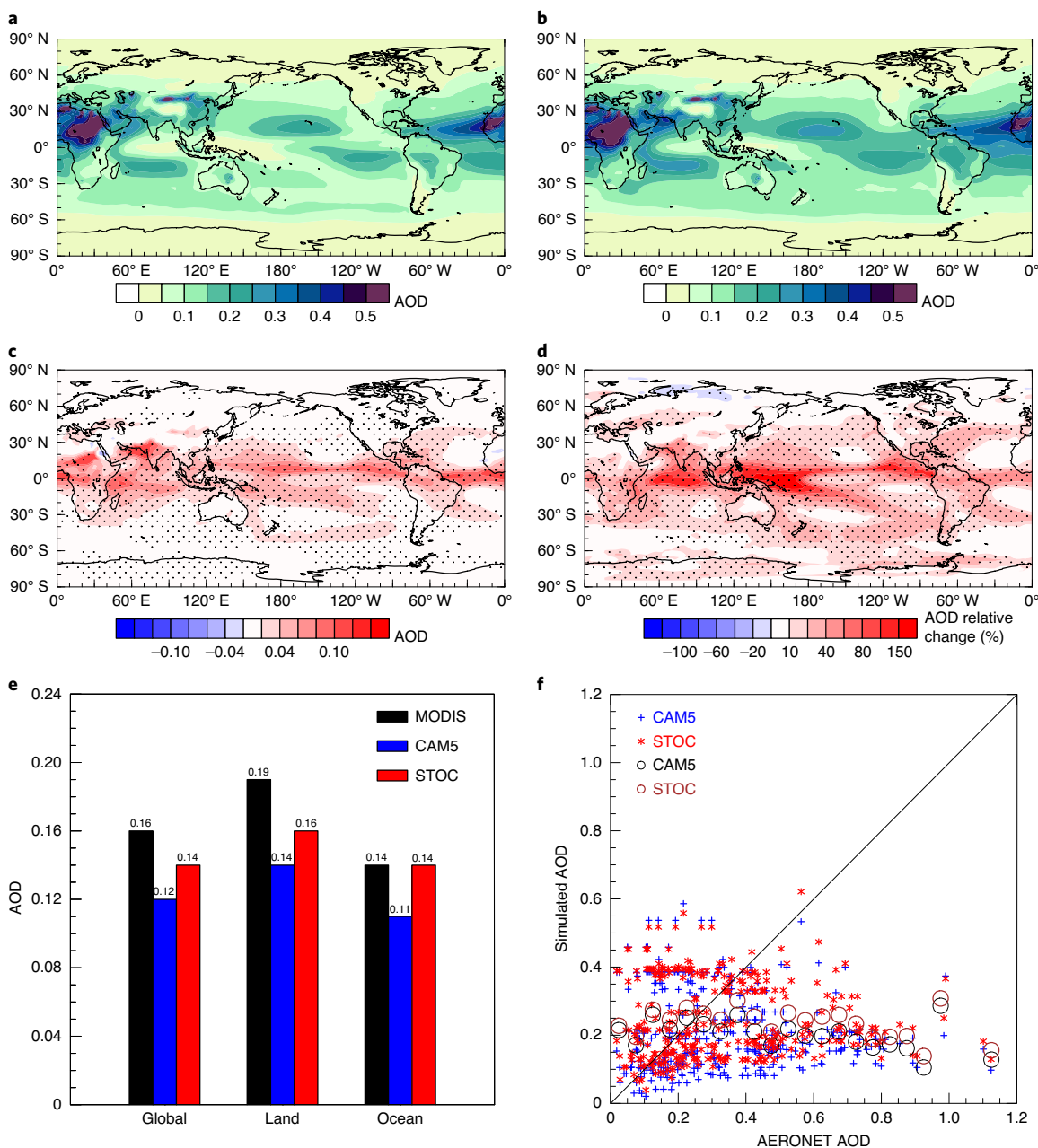


Fig. 3 | AOD at 550 nm. **a, b**, Global distributions of AOD in CAM5 (**a**) and STOC (**b**) simulations. **c**, Absolute AOD changes from CAM5 to STOC simulations. **d**, AOD relative change (%) from CAM5 to STOC simulations. **e**, AOD means over the globe, land and ocean for MODIS, CAM5 and STOC. **f**, Observed and simulated AOD at AERONET sites over 30°S–30°N. Large circles in **f** represent the modelled AOD average in each AERONET observed AOD bin with an interval of 0.05. Areas exceeding 95% *t*-test confidence level in **c** and **d** are stippled.

aerosol wet removal is slightly less in absolute amount (from 12.0 to 10.0 $\text{mg m}^{-2} \text{d}^{-1}$). For individual aerosol species, the results are similar (Extended Data Figs. 4 and 5), as they are for EAMv1 (Extended Data Figs. 6 and 7). The reduced light-rain frequency has a huge impact on aerosol wet removal. In terms of the absolute amount, the aerosol wet removal by rainfall rates $<10 \text{ mm d}^{-1}$ is reduced from 14.48 ($=77\% \times 18.8$) $\text{mg m}^{-2} \text{d}^{-1}$ to 10.14 ($=63\% \times 16.1$) $\text{mg m}^{-2} \text{d}^{-1}$, a relative reduction of 43% of wet removal by light rain of $<10 \text{ mm d}^{-1}$.

Increased aerosol optical depth

The geographical distributions of aerosol optical depth (AOD) in Moderate Resolution Imaging Spectroradiometer (MODIS) and Aerosol Robotic Network (AERONET) observations and

simulations (Fig. 3a,b and Supplementary Fig. 1) all show high AOD over land and low AOD over oceans. Due to the reduced wet removal by light rain, the AOD is increased almost globally, especially over the tropics and subtropics, by up to 0.3 in tropical rain belts (Fig. 3c). This translates to a relative increase of more than 100% in the intertropical convergence zone (Fig. 3d), where rain is predominantly of a convective nature. Aerosol burdens from individual aerosol species, especially sea salt and sulfate, also increase in tropical precipitation regions (Supplementary Fig. 2). Consequently, the lifetimes (defined as burden divided by total (dry plus wet) removal rate) of individual aerosols are prolonged (Extended Data Fig. 8), by percentages varying from 7.3% for sulfate to 16.7% for sea salt. The changes and improvements in the EAMv1 simulations are

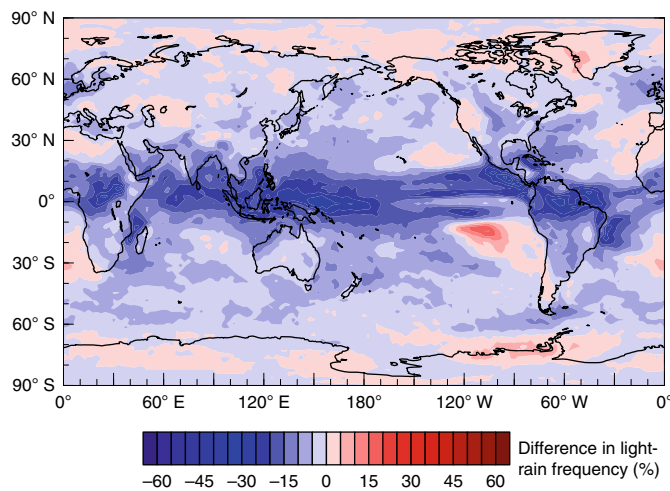


Fig. 4 | Changes of light-rain frequency. Global distribution of differences in light-rain ($1 < P < 20 \text{ mm d}^{-1}$) frequency between the CAM5 and STOC simulations (STOC minus CAM5).

qualitatively similar but with a smaller magnitude (Supplementary Figs. 3 and 4).

On global average or averaging over land and oceans separately, the underestimation of AOD compared with MODIS is alleviated (Fig. 3e) with the reduction of light rainfall. The global mean AOD is increased by nearly 17% from 0.12 to 0.14 (14% for land average and 27% for ocean average). The relative reduction of the mean bias is 50% globally (from -0.04 to -0.02), 40% over land and 100% over oceans. This suggests that the oversimulated light-rain frequency may be an important missing cause of the negative AOD biases common in GCMs. Compared with AERONET observations, the model simulations severely underestimate the AOD for high AOD values but overestimate it for low AOD values in all latitude zones (Fig. 3f and Extended Data Fig. 9). Despite this, the STOC simulations consistently have smaller biases than the CAM5 simulations.

The global distribution of the AOD increase highly resembles the pattern of decrease in light-rain ($1 < P < 20 \text{ mm d}^{-1}$ (ref. 27)) frequency (Fig. 4), with a correlation coefficient of -0.7 at a significance level greater than 99%, again demonstrating the dominant role of light-rain frequency in aerosol response. By contrast, the spatial distribution of changes in total, convective and large-scale rainfall amount has no similarity to the AOD change pattern (Extended Data Fig. 10). In fact, in the tropical rain belts where the maximum increase of AOD exists, the total, convective and large-scale rainfall amounts all increase, which, if anything, would reduce AOD.

The aerosol wet removal is predominantly through scavenging by light rain. By reducing the frequency of light rain in two GCMs, we find that the aerosol burden in the atmosphere is increased substantially, by 17% for global mean AOD. Thus, light rainfall has a disproportionate control on aerosol burden. The common problem of too much light rain and too little heavy rain in GCMs may be an important missing cause for the underestimation of aerosol burden. In future climate projections, although precipitation is expected to increase, its impact on aerosol concentration in the atmosphere will critically depend on how the occurrence of light rain changes. Aerosol radiative effect is a major source of uncertainties in climate change projections. Therefore, the findings in this study have profound implications for understanding the nature of aerosol–climate interaction and its impact on climate.

Online content

Any methods, additional references, Nature Research reporting summaries, source data, extended data, supplementary information,

acknowledgements, peer review information; details of author contributions and competing interests; and statements of data and code availability are available at <https://doi.org/10.1038/s41561-020-00675-z>.

Received: 27 April 2020; Accepted: 26 November 2020;

Published online: 11 January 2021

References

- Abdul-Razzak, H. & Ghan, S. J. A parameterization of aerosol activation: 2. multiple aerosol types. *J. Geophys. Res. Atmos.* **105**, 6837–6844 (2000).
- Wang, Y., Liu, X., Hoose, C. & Wang, B. Different contact angle distributions for heterogeneous ice nucleation in the Community Atmospheric Model version 5. *Atmos. Chem. Phys.* **14**, 10411–10430 (2014).
- Wang, Y. & Liu, X. Immersion freezing by natural dust based on a soccer ball model with the Community Atmospheric Model version 5: climate effects. *Environ. Res. Lett.* **9**, 124020 (2014).
- Carlsaw, K. et al. A review of natural aerosol interactions and feedbacks within the Earth system. *Atmos. Chem. Phys.* **10**, 1701–1737 (2010).
- Raes, F., Liao, H., Chen, W. T. & Seinfeld, J. H. Atmospheric chemistry–climate feedbacks. *J. Geophys. Res. Atmos.* **115**, D12121 (2010).
- Myhre, G. et al. in *Climate Change 2013: The Physical Science Basis* (eds Stocker, T. F. et al.) Ch. 8 (IPCC, Cambridge Univ. Press, 2013).
- Boucher, O. et al. in *Climate Change 2013: The Physical Science Basis* (eds Stocker, T. F. et al.) 571–657 (IPCC, Cambridge Univ. Press, 2013).
- Forouzanfar, M. H. et al. Global, regional, and national comparative risk assessment of 79 behavioural, environmental and occupational, and metabolic risks or clusters of risks in 188 countries, 1990–2013: a systematic analysis for the Global Burden of Disease Study 2013. *Lancet* **386**, 2287–2323 (2015).
- Xing, Y., Xu, Y., Shi, M. & Lian, Y. The impact of $\text{PM}_{2.5}$ on the human respiratory system. *J. Thorac. Dis.* **8**, 69–74 (2016).
- Chowdhury, S., Dey, S. & Smith, K. R. Ambient $\text{PM}_{2.5}$ exposure and expected premature mortality to 2100 in India under climate change scenarios. *Nat. Commun.* **9**, 318 (2018).
- Park, S., Allen, R. J. & Lim, C. H. A likely increase in fine particulate matter and premature mortality under future climate change. *Air Qual. Atmos. Health* **13**, 143–151 (2020).
- Silva, R. A. et al. Future global mortality from changes in air pollution attributable to climate change. *Nat. Clim. Change* **7**, 647–651 (2017).
- Rasch, P. J., Barth, M. C., Kiehl, J. T., Schwartz, S. E. & Benkovitz, C. M. A description of the global sulfur cycle and its controlling processes in the National Center for Atmospheric Research community climate model, version 3. *J. Geophys. Res. Atmos.* **105**, 1367–1385 (2000).
- Jacob, D. J. & Winner, D. A. Effect of climate change on air quality. *Atmos. Environ.* **43**, 51–63 (2009).
- Fang, Y. et al. The impacts of changing transport and precipitation on pollutant distributions in a future climate. *J. Geophys. Res. Atmos.* **116**, D18303 (2011).
- Mahowald, N., Albani, S., Engelstaedter, S., Winckler, G. & Goman, M. Model insight into glacial–interglacial paleodust records. *Quat. Sci. Rev.* **30**, 832–854 (2011).
- Racherla, P. N. & Adams, P. J. Sensitivity of global tropospheric ozone and fine particulate matter concentrations to climate change. *J. Geophys. Res. Atmos.* **111**, D24103 (2006).
- Avise, J. et al. Attribution of projected changes in summertime US ozone and $\text{PM}_{2.5}$ concentrations to global changes. *Atmos. Chem. Phys.* **9**, 1111–1124 (2009).
- Kirtman, B. et al. in *Climate Change 2013: The Physical Science Basis* (eds Stocker, T. F. et al.) 953–1028 (IPCC, Cambridge Univ. Press, 2013).
- Ackerley, D., Highwood, E. J., Frame, D. J. & Booth, B. B. Changes in the global sulfate burden due to perturbations in global CO_2 concentrations. *J. Clim.* **22**, 5421–5432 (2009).
- Kloster, S. et al. A GCM study of future climate response to aerosol pollution reductions. *Clim. Dyn.* **34**, 1177–1194 (2010).
- Xu, Y. & Lamarque, J.-F. Isolating the meteorological impact of 21st century GHG warming on the removal and atmospheric loading of anthropogenic fine particulate matter pollution at global scale. *Earths Future* **6**, 428–440 (2018).
- Allen, R. J., Landuyt, W. & Rumbold, S. T. An increase in aerosol burden and radiative effects in a warmer world. *Nat. Clim. Change* **6**, 269–274 (2016).
- Allen, R. J., Hassan, T., Randles, C. A. & Su, H. Enhanced land–sea warming contrast elevates aerosol pollution in a warmer world. *Nat. Clim. Change* **9**, 300–305 (2019).
- Golaz, J.-C. et al. Sensitivity of the aerosol indirect effect to subgrid variability in the cloud parameterization of the GFDL atmosphere general circulation model AM3. *J. Clim.* **24**, 3145–3160 (2011).
- Jing, X. & Suzuki, K. The impact of process-based warm rain constraints on the aerosol indirect effect. *Geophys. Res. Lett.* **45**, 10729–10737 (2018).

27. Na, Y., Fu, Q. & Kodama, C. Precipitation probability and its future changes from a global cloud-resolving model and CMIP6 simulations. *J. Geophys. Res. Atmos.* **125**, e2019JD031926 (2020).
28. Wang, Y., Zhang, G. J. & Craig, G. C. Stochastic convective parameterization improving the simulation of tropical precipitation variability in the NCAR CAM5. *Geophys. Res. Lett.* **43**, 6612–6619 (2016).
29. Wang, Y., Zhang, G. J. & He, Y. J. Simulation of precipitation extremes using a stochastic convective parameterization in the NCAR CAM5 under different resolutions. *J. Geophys. Res. Atmos.* **122**, 12875–12891 (2017).
30. Wang, Y., Zhang, G. J. & Jiang, Y. J. Linking stochasticity of convection to large-scale vertical velocity to improve Indian summer monsoon simulation in the NCAR CAM5. *J. Clim.* **31**, 6985–7002 (2018).
31. Dai, A. Precipitation characteristics in eighteen coupled climate models. *J. Clim.* **19**, 4605–4630 (2006).
32. Deng, Y., Bowman, K. P. & Jackson, C. Differences in rain rate intensities between TRMM observations and community atmosphere model simulations. *Geophys. Res. Lett.* **34**, L01808 (2007).
33. Wang, Y. & Zhang, G. J. Global climate impacts of stochastic deep convection parameterization in the NCAR CAM 5. *J. Adv. Model. Earth Syst.* **8**, 1641–1656 (2016).

Publisher's note Springer Nature remains neutral with regard to jurisdictional claims in published maps and institutional affiliations.

© The Author(s), under exclusive licence to Springer Nature Limited 2021